Comparative Investigation of InGaP/GaAs/GaAsBi and InGaP/GaAs Heterojunction Bipolar Transistors

© Yi-Chen Wu*, Jung-Hui Tsai+¶, Te-Kuang Chiang*, Fu-Min Wang*

* Department of Electrical Engineering, National University of Kaohsiung, 700, Kaohsiung University Rd., 811 Kaohsiung, Taiwan
+ Department of Electronic Engineering, National Kaohsiung Normal University, 802 Kaohsiung, Taiwan

(Получена 4 февраля 2015 г. Принята к печати 16 марта 2015 г.)

In this article the characteristics of $In_{0.49}Ga_{0.51}P/GaAs/GaAs_{0.975}Bi_{0.025}$ and $In_{0.49}Ga_{0.51}P/GaAs$ heterojunction bipolar transistor (HBTs) are demonstrated and compared by two-dimensional simulated analysis. As compared to the traditional InGaP/GaAs HBT, the studied InGaP/GaAs/GaAsBi HBT exhibits a higher collector current, a lower base-emitter ($B-E$) turn-on voltage, and a relatively lower collector-emitter offset voltage of only 7 mV. Because the more electrons stored in the base is further increased in the InGaP/GaAs/GaAsBi HBT, it introduces the collector current to increase and the $B-E$ turn-on voltage to decrease for low input power applications. However, the current gain is slightly smaller than the traditional InGaP/GaAs HBT attributed to the increase of base current for the minority carriers stored in the GaAsBi base.

1. Introduction

GaAs-based heterojunction bipolar transistors (HBTs) have widely used as key devices on microwave circuit due to their superior carrier transport properties [1,2]. However, the turn-on voltage difference between base-emitter ($B-E$) heterojunction and base-collector ($B-C$) homojunction still is a significant factor to cause a large collector-emitter ($C-E$) offset voltage (ΔV_{CE}), which will substantially increase unnecessary power consumption in circuit applications [3]. For the requirement of low input power, InP-based HBTs are useful for the small energy-gap InGaAs material generally employed as the base layer. Nevertheless, InP substrates are expensive, fragile and easily broken during processing than the transistors based on GaAs substrates. Therefore, the development of HBTs with a small energy-gap InGaAs base grown on GaAs substrates has attracted significant interest for the low cost and low input power [4]. Nevertheless, the thickness of InGaAs base layer is severely limited due to the lattice mismatch with the GaAs layer [5].

Among of the GaAs-based HBTs, InGaP/GaAs has been a dominated material system for high-speed semiconductor devices because of the low DX center density, low surface recombination velocity, high etching selectively between InGaP and GaAs material layers, and high ratio of valence band discontinuity ($\Delta E_V \approx 0.3$ eV) to conduction band discontinuity ($\Delta E_C \approx 0.2$ eV) at heterojunction [4,6,7]. The hole confinement effect of InGaP/GaAs HBTs is good for the larger ΔE_V value at $B-E$ heterojunction. Moreover, the considerable ΔE_C will introduce a potential barrier for electron injection from emitter into base and then it will cause a large $C-E$ offset voltage. Recently, another material system, i. e., InGaP/GaAs/GaAsBi, has a significant potential for high-performance HBTs attributed that the band-gap discontinuity is almost equal to the ΔE_V at GaAs/GaAsBi heterojunction [8–10]. The $GaAs_{1-x}Bi_x$ layer with low

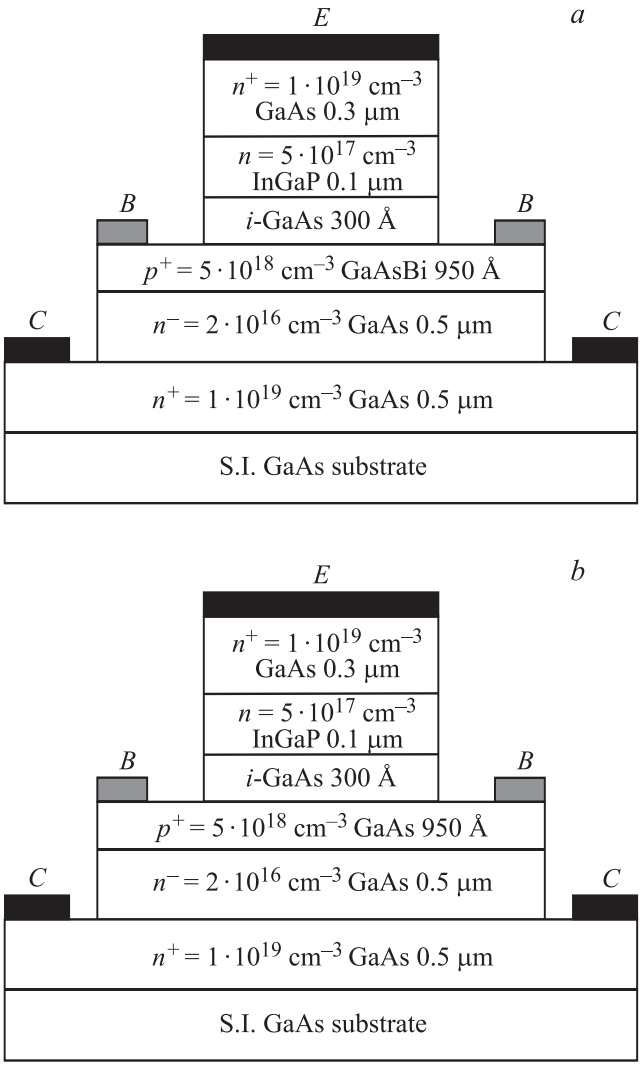

Figure 1. Schematic cross sections of the (a) device A and (b) device B.

¶ E-mail: jhtsai@nknucc.nknu.edu.tw

mismatch had been grown on GaAs substrates with Bi concentrations between 0 and 5% and up to 12% [9]. In particular, the incorporation of Bi atoms into GaAs, i. e., $GaAs_{1-x}Bi_x$, only alters the valence band and shrink the energy gap of GaAs, while the electron mobility and conduction band are unchanged [8]. However, though $GaAs_{1-x}Bi_x$ material could be acted as a base layer for the narrow energy gap, the difference of device characteristics between $GaAs_{1-x}Bi_x$ and GaAs base layers have not reported until now.

In this article, the performance of InGaP/GaAs/GaAsBi and InGaP/GaAs HBTs is comparatively demonstrated. As compared with the conventional InGaP/GaAs HBT, the simulated results exhibits that the InGaP/GaAs/GaAsBi HBT with a smaller energy-gap GaAsBi base layer has a higher collector current and a lower $B-E$ turn-on voltage for the potential application on low input-power signal amplifiers and circuits.

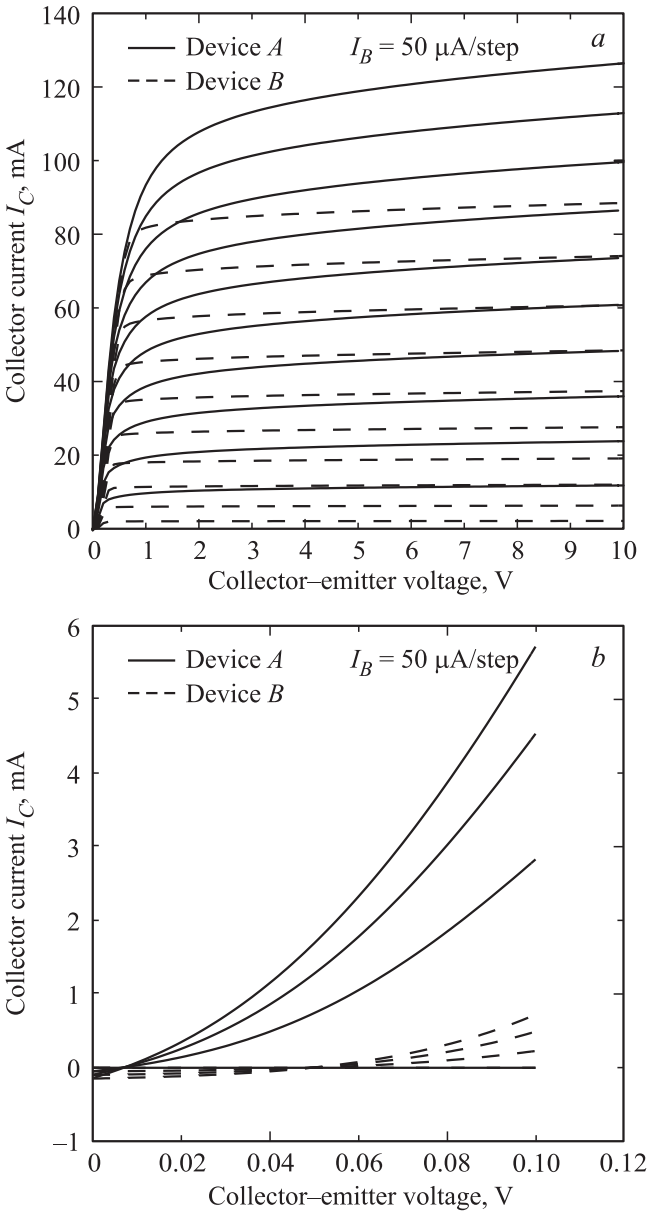

Figure 2. *a* — common-emitter current-voltage characteristics at room temperature of devices *A* and *B*; *b* — enlarged view near the origin of the current-voltage characteristics.

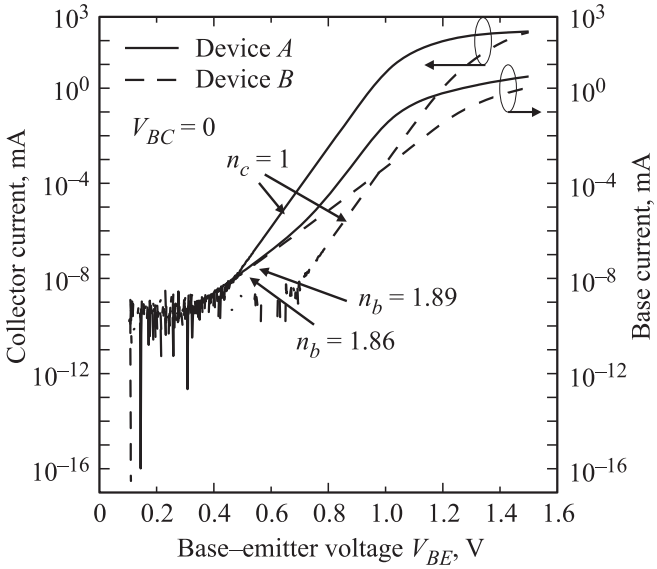

Figure 3. Gummel plots of devices *A* and *B* at $V_{BC} = 0$.

2. Device structures

The device structure of the studied InGaP/GaAs/GaAsBi HBT (labeled device *A*) includes a 5000 Å $n^+ = 10^{19}$ cm^{-3} GaAs subcollector layer, a 5000 Å $n^- = 2 \cdot 10^{16}$ cm^{-3} GaAs collector layer, a 950 Å $p^+ = 5 \cdot 10^{18}$ cm^{-3} $GaAs_{0.975}Bi_{0.025}$ bulk base layer, a 300 Å undoped GaAs spacer layer, a 1000 Å $n = 5 \cdot 10^{17}$ cm^{-3} $In_{0.49}Ga_{0.51}P$ emitter layer, and a 3000 Å $n^+ = 10^{19}$ cm^{-3} GaAs cap layer. For comparison, the conventional InGaP/GaAs HBT (labeled device *B*), has the similar structure as the device A except that a 950 Å $p^+ = 5 \cdot 10^{18}$ cm^{-3} GaAs bulk base layer is employed to replace the GaAsBi base layer. A two-dimensional ($2D$) semiconductor simulation package SILVACO was used to analyze the energy band, distributions of electrons and holes, and *DC* performance of the two devices [11]. The $2D$ analysis takes into account the Poisson equation, continuity equation of electrons and holes, Shockley–Read–Hall (SRH) recombination, Auger recombination, and Boltzmann statistics, simultaneously. Fig. 1 illustrates the schematic cross sections of the devices *A* and *B*, respectively. The emitter and collector areas are 50×50 and $100 \times 100\,\mu$m, respectively.

3. Results and discussion

The common-emitter current-voltage ($I-V$) characteristics of the two devices at room temperature are shown in Fig. 2, *a*. The base currents I_B are applied by 50 μA/step.

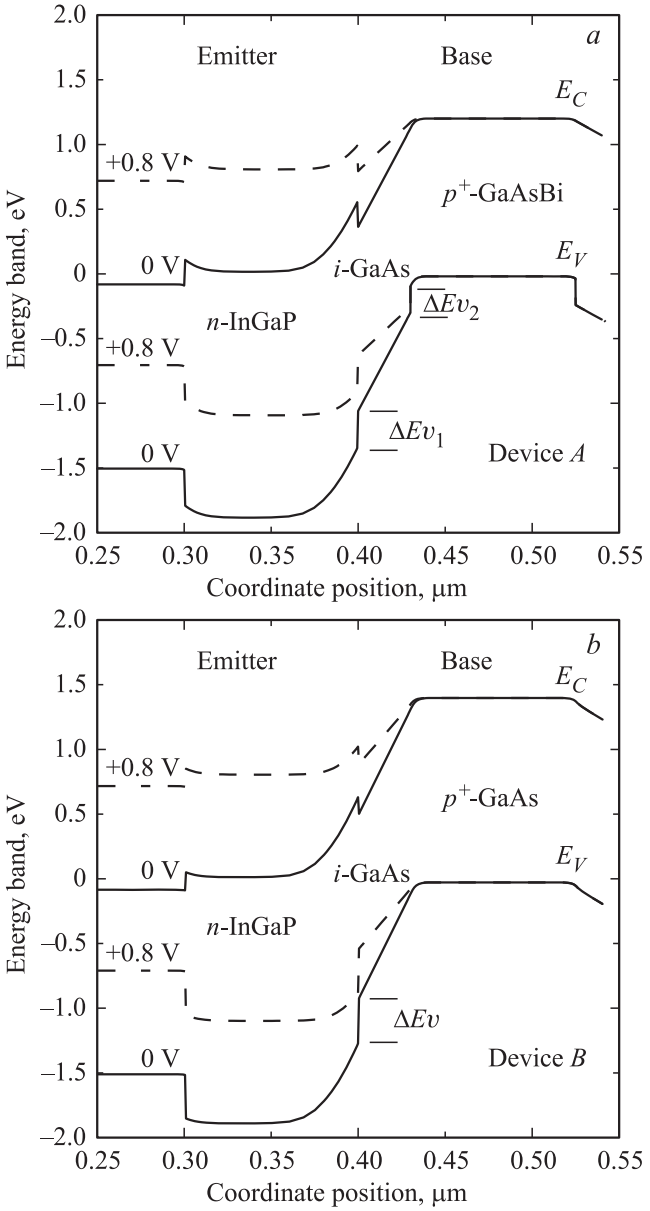

Figure 4. Energy band diagrams near base-emitter junction at $V_{BE} = 0$ and $+0.8$ V of the (a) device A and (b) device B.

Clearly, the device A exhibits a higher current than the device B. An enlarged view near the origin of the $I-V$ characteristics is depicted in Fig. 2, b. As seen in the figure, a relatively low $C-E$ offset voltage of only 7 mV at $I_B = 50\,\mu$A is observed in the device A, while the device B shows a larger value of about 50 mV. Fig. 3 depicts the Gummel plots of the devices at $V_{BC} = 0$ V. At collector current level of $1\,\mu$A, the $B-E$ turn-on voltage of the device A is only 0.77 V, which is lower than that of 1.01 V in the device B. The low $B-E$ turn-on voltage of the device A can reduce the input voltage and $C-E$ offset voltage for substantially decreasing the power consumption in circuit applications. Though the maximum current gain of 154 in the device A is lightly smaller than that of 206 in the device B, it exhibits a relatively low $B-E$ input voltage of 0.445 V as the current gain is unity. In both devices, the ideality factors n_c of collector currents are near equal to unity at low current level. This means that the diffusion mechanism dominates the electron transportation across the $E-B$ junction and the potential spike at this $B-E$ junction has been eliminated. On the other hand, the ideality factors n_b of base currents are of about 1.86 and 1.89 at low current level for the devices A and B, respectively, which denotes that recombination dominates the total base currents and the difference of the two devices is small at this current level. The characteristic comparison of the devices with $GaAs_{0.975}Bi_{0.025}$ and GaAs bases will be explained as follows.

The energy band diagrams near the $B-E$ junction at equilibrium and under forward $B-E$ bias for the devices A and B are plotted in Figs. 4, a and b, respectively. Obviously, the potential spikes at $B-E$ junction of the both devices are completely eliminated, even at $V_{EB} = +0.8$ V. The employ-

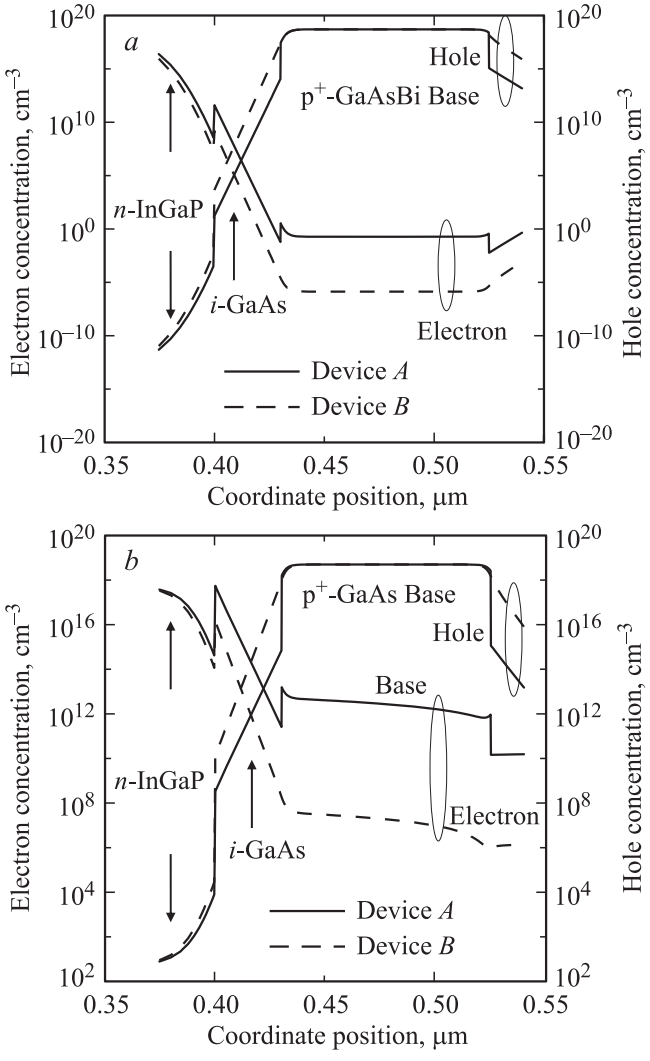

Figure 5. Charge distributions near the base-emitter junction (a) at $V_{BE} = 0$ and (b) at $V_{BE} = +0.8$ V.

ment of a 300 Å undoped GaAs spacer layer between the n-InGaP emitter and p^+-GaAs (and p^+-$GaAs_{0.975}Bi_{0.025}$) base layers can enable the $p-n$ junction to act as a homojunction, and it helps to lower the energy band at emitter side for eliminating the potential spike and reducing the offset voltage. The charge distributions near the $B-E$ junction at $V_{BE} = 0$ and $+0.8$ V are depicted in Figs. 5, *a* and *b*, respectively. In the device *A*, due to the presence of another ΔE_V at GaAs/GaAsBi heterojunction, it will strengthen the confinement effect for holes at $B-E$ junction and the hole concentrations in the i-GaAs spacer and n-InGaP emitter region are sufficiently suppressed as compared with the device *B*. Nevertheless, it is worthy to note that the electron (minority carrier) concentration in the base region of the device *A* is higher when compared with the device *B*, which can be attributed to the higher intrinsic concentration n_i of the GaAsBi base layer at the same base doping concentration, as seen in Figs. 5, *a* and *b*. This will substantially cause the $1\,kT$ base bulk recombination current and total base current to slightly increase. Thus, the ideality factor n_b of device *A* is somewhat small than the device *B* at low current level. On the other hand, the more electrons stored in the p^+-GaAsBi base layer could promote the collector current. In general, the minority carrier (electrons) Q_n in the base region can be given by

$$Q_n = \tau_n J_n(x_p), \qquad (1)$$

where τ_n is lifetime of minority carriers, and $J_n(x_p)$ is the electron current density at the depletion boundary of pn junction at p-type base side. According to the above equation, the more minority carriers in the base will result in the emitter (and collector) current to increase and the $B-E$ turn-on voltage to decrease. Therefore, the device *A* exhibits a higher collector current and a lower $B-E$ turn-on voltage when the current gain is unity.

4. Conclusion

We have successfully demonstrated the characteristic difference of $In_{0.49}Ga_{0.51}P$/GaAs/$GaAs_{0.975}Bi_{0.025}$ and $In_{0.49}Ga_{0.51}P$/GaAs HBTs. Attributed to the different of minority carrier stored in the $GaAs_{0.975}Bi_{0.025}$ and GaAs base region, obvious variation in device characteristics are observed. As compared with the traditional InGaP/GaAs HBT, The studied InGaP/GaAs/GaAsBi HBT exhibits a higher collector current, a lower turn-on voltage, a lower $C-E$ offset voltage, and a somewhat lower current gain. Consequentially, the demonstration and comparison of the studied transistors provide a promise for application in low-power consumption circuits.

Acknowledgement. This work is supported by the Ministry of Science and Technology of the Republic of China under Contract No. MOST 103-2221-E-017-013.

References

[1] P.M. Asbeck, M.F. Chang, K.C. Wang, G.J. Sullivan, D.T. Cheung. Proc. IEEE, **81**, 1709 (1993).
[2] K. Runge, P.J. Zampardi, R.L. Pierson, P.B. Thomas, S.M. Beccue, R. Yu, K.C. Wang. *IEEE GaAs IC Symposium* (1997) c. 211.
[3] S.I. Fu, T.P. Chen, R.C. Liu, S.Y. Cheng, P.H. Lai, Y.Y. Tsai, C.W. Hung, W.C. Liu. J. Electrochem. Soc., **154**, H289 (2007).
[4] J.H. Tsai, Y.H. Lee, N.F. Dale, J.S. Sheng, Y.C. Ma, S.S. Ye. Appl. Phys. Lett., **96**, 063 505 (2010).
[5] D.A. Ahmari, M.T. Fresina, Q.J. Hartmann, D.W. Barlage, P.J. Mares, M. Feng. IEEE Electron. Dev. Lett., **17**, 226 (1996).
[6] S.S. Lu, C.C. Hung. IEEE Electron. Dev. Lett., **13**, 214 (1992).
[7] J.H. Tsai, C.S. Lee, W.S. Lour, Y.C. Ma, S.S. Ye. Semiconductors, **45**, 646 (2011).
[8] G. Pettinari, A. Polimeni, M. Capizzi, J.H. Blokland, P.C.M. Christianen, J.C. Maan, E.C. Young, T. Tiedje. Appl. Phys. Lett., **92**, 262 105 (2008).
[9] A.J. Ptak, R. France, D.A. Beaton, K. Alberi, J. Simon, A. Mascarenhas, C.S. Jiang. J. Cryst. Growth, **338**, 107 (2012).
[10] Z.D. Marks. IEEE Trans. Electron Dev., **60**, 200 (2013).
[11] SILVACO 2013 Atals User's Manual Editor I (SILVACO Int. Santa Clara, CA, USA)

Редактор Т.А. Полянская